*Bulgarian Chemical Communications, Volume 50, Special Issue G (pp. 68 - 77) 2018*

# Investigation of the different Reynolds numbers influence on the atomization and combustion processes of liquid fuel

A.S. Askarova[1], S.A. Bolegenova[1*], V.Yu. Maximov[1], S.A. Bolegenova[1], Sh.S. Ospanova[1], M.T. Beketayeva[1], A.O. Nugymanova[1], N.V. Pilipenko[2], Zh.K. Shortanbayeva[1], K.S. Baktybekov[3], A.B. Syzdykov[1]

[1] *Al-Farabi Kazakh National University, Department of Thermal and Technical Physics, Al-Farabi ave. 71, Kazakhstan*

[2] *Saint-Petersburg national research University of information technologies, mechanics and optics, Saint-Petersburg, Russia*

[3] *«National Company «Kazakhstan Gharysh Sapary» JSC*

The problems of combustion are widely studied now by the scientists of the world. Increasing level of ecological pollution of the environment, reserve depletion of hydrocarbon fuel and economic growth of many countries causing increase of demand for energy - all these factors gave rise to the problem of finding of more economic and ecological way of fuel combustion. In order to solve this problem it is necessary to study thoroughly the combustion process itself and that is why the methods of numerical simulation are getting wide spread in the science. The turbulence plays great role in many devices using combustion process and its study is maybe one of the most complicated sections of hydrodynamics. It is also necessary to take into account additional factors such as various chemical reactions and radiation.

In this article tetradecane's combustion depending on the Reynolds numbers of the gas flow are investigated. Reynolds numbers of the gas flow was ranging from 2300 to 25000. As the result of the conducted numerical experiments it has been determined that at high Reynolds numbers the combustion process occurs intensively. The most effective combustion proceeds at the Reynolds number of the gas flow equal 25000, under these conditions temperature reaches values from 2001 K to 2645 K. With this value of the Reynolds number, the combustion temperature in the combustion chamber reaches maximum values and intensive evaporation of the liquid fuel drops begins. It was shown that when the Reynolds number is 15,000 and 20,000, the concentration of emitted carbon dioxide reaches the average allowable values, which are equal to $0{,}104823 \cdot 10^{-3}$ kg/kg and $0{,}104747 \cdot 10^{-3}$ kg/kg respectively.

**Keywords:** numerical simulation, combustion, two-phase flows, Reynolds number, tetradecane, modeling.

## INTRODUCTION

One of the priority tendencies of the scientific and technological development of Kazakhstan is the research of simulation of formation of polluting fog and their dispersion in the atmosphere. This problem has a great value because of the increasing concern for the ecological situation in Kazakhstan as the atmospheric air in the cities of Kazakhstan is daily polluted by different hazardous substances ($NO_2$, CO, $CO_2$, soot and so on) [1-5].

For the recent years the dispersion of the liquid sprays in the neutral atmospheric flows has been well studied by means of numerical, laboratory and natural researches. In these researches the main attention has been given to the dispersion of chemically reactive scalar admixture in the free convective flows.

As a matter of urgency, the use of liquid fuels can be said that over the past few years 60 million passenger cars have been produced, that is, 165,000 vehicles are produced per day. The engines of the current generation are significantly different from those used a few decades ago. The main combustion process in engines remains the same, but the types of injections differ significantly. For example, modern engines with electronically controlled injection systems, along with air compression mechanisms that help improve the combustion process, use only the required amount of fuel. More than 50% of cars are produced in Asia and Oceania, while Europe produces almost a third of the total number of cars in the world. In the last decade, the total number of cars produced per year has increased by 20 million, which leads to a high growth of pollutants that pose a greater threat to the environment [6-11].

The regulations on emissions of pollutants are becoming more and more severe over time, for example, until 2025, due to world-wide established ground rules, it is planned to reduce $CO_2$ emissions from passenger cars to about 100 mg per km. It is known that the International Energy Agency (IEA) has been tasked to use renewable energy sources as an energy carrier by 2050 and to reduce $CO_2$ emissions to the atmosphere by half as an indicator of harmful substances [12-14].

Although carbon dioxide is not a toxic gas, it still represents a danger to the environment due to

* To whom all correspondence should be sent:
Saltanat.Bolegenova@kaznu.kz

the greenhouse effect. According to estimates [15], the annual carbon footprint is about 30 billion tons due to various types of human activity around the world. The concentration of carbon dioxide from all sources has increased by 31% since 1750 [16].

The investigation of the formation of polluting fog will allow creating the methods for the decrease of contain of hazardous substances in the atmosphere and for the prevention of formation of such clouds which contain hot liquid particles and these particles are the reasons of the formation of such polluting fog. That kind of problems is one of the significant and insufficiently explored tasks for the present days.

In this region of research the numerical experiments on the combustion of liquid fuel sprays in the burner chamber have been carried out. In this work it has been researched the dependence of maximal temperature of combustion of the liquid fuel from the velocity of the spray by means of the numerical modeling on the basis of the solution of differential two-dimensional equations of the turbulent reactive flows.

## MATHEMATICAL MODEL OF THE PROBLEM

Main equations of mathematical model of atomization and combustion of spray of liquid fuel are presented below [17-20].

Continuity equation for component *m*:

$$\frac{\partial \rho_m}{\partial t} + \vec{\nabla}(\rho_m \vec{u}) = \vec{\nabla}\left[\rho D \vec{\nabla}\left(\frac{\rho_m}{\rho}\right)\right] + \dot{\rho}_m^c + \dot{\rho}^s \delta_{m1}. \quad (1)$$

Where $\rho_m$ - mass density of the liquid phase, $\rho$ - total mass density, u - fluid velocity, D - diffusion coefficient, $\nabla$ - Nabla operator, $\dot{\rho}_m^c$ - chemical source term, $\dot{\rho}^s$ - source term due to injection, $\delta$ - Kronecker symbol.

Momentum equation:

$$\frac{\partial(\rho\vec{u})}{\partial t} + \vec{\nabla}(\rho\vec{u}\vec{u}) = -\frac{1}{a^2}\vec{\nabla}p - A_0\vec{\nabla}\left(\frac{2}{3}\rho k\right) + \vec{\nabla}\vec{\sigma} + \vec{F}^s + \rho\vec{g}. \quad (2)$$

Where p - fluid pressure, $\alpha$ - immeasurable value used in the PGS method. This is a method that allows one to increase computational efficiency in low Mach number flows, where the pressure is approximately uniform. $A_0$ is 0 in the case of laminar flow, and 1, when one of the turbulence models is used. In our studies, we used the method of modeling the turbulent flows of RANS, which is based on the Boussinesq hypothesis and implies a time averaging of the Navier-Stokes equation. Also $\sigma$ is viscous stress tensor, which depends on the viscosity of the fluid and the specific internal energy. The value $\vec{F}^s$ on the right side of the equation denote external forces that affect the mass and the volume of the fluid.

Energy equation:

$$\frac{\partial(\rho I)}{\partial t} + \vec{\nabla}(\rho\vec{u}I) = -p\vec{\nabla}\vec{u} + (1-A_0)\sigma\vec{\nabla}\vec{u} - \vec{\nabla}\vec{J} + A_0\rho\varepsilon + \dot{Q}^c + \dot{Q}^s, \quad (3)$$

where heat flux vector consists of electrical conductivity and enthalpy transfer:

$$\vec{J} = -K\nabla T - \rho D\sum_m h_m \nabla\left(\frac{\rho_m}{\rho}\right)$$

and $\dot{Q}^c$ - source term due to heat generated by a chemical reaction, $\dot{Q}^s$ - the heat that brings the injected fuel, $\varepsilon$ - dissipation of the kinetic energy of turbulence.

More universal models in engineering calculations of turbulent flows are models with two differential equations. This is a $k-\varepsilon$ model, when two equations are solved for the kinetic energy of turbulence $k$ and its dissipation rate $\varepsilon$. Equations of $k-\varepsilon$ turbulence model [21-26]:

$$\frac{\partial\rho k}{\partial t} + \vec{\nabla}(\rho\vec{u}k) = -\frac{2}{3}\rho k\vec{\nabla}\vec{u} + \vec{\sigma}:\vec{\nabla}\vec{u} + \vec{\nabla}\left[\left(\frac{\mu}{\mathrm{Pr}_k}\right)\vec{\nabla}k\right] - \rho\varepsilon + \dot{W}^s. \quad (4)$$

$$\frac{\partial\rho\varepsilon}{\partial t} + \vec{\nabla}(\rho\vec{u}\varepsilon) = -\left(\frac{2}{3}c_{\varepsilon_1} - c_{\varepsilon_3}\right)\rho\varepsilon\vec{\nabla}\vec{u} + \vec{\nabla}\left[\left(\frac{\mu}{\mathrm{Pr}_\varepsilon}\right)\vec{\nabla}\varepsilon\right] + \frac{\varepsilon}{k}\left[c_{\varepsilon_1}\vec{\sigma}:\vec{\nabla}\vec{u} - c_{\varepsilon_2}\rho\varepsilon + c_s\dot{W}^s\right] \quad (5)$$

When calculating various flow characteristics, a system of turbulent transfer equations was used, for

closure of which a standard $k-\varepsilon$ model of turbulence was used, since this model exhibits stability, efficiency, and reasonable accuracy in studies of heat and mass transfer processes in turbulent flows of liquid fuels, which makes it most suitable for solving industrial problems.

*Initial and boundary conditions of the problem of atomization and combustion of liquid fuels in the combustion chamber*

At the initial moment of time, the gas in the combustion chamber is at rest and the initial temperature distribution is constantly:

$t=0: u=0,\ v=0,\ w=0,\ T=T_0,\ c=c_0.$

The velocity field at the wall is determined through the turbulent law of the wall, and the velocity component profiles are given by the logarithmic distribution:

$$\frac{\upsilon}{u^*}=\begin{cases}1/\mathrm{k}\ln\left(c_{l\omega}\zeta^{7/8}\right), & \zeta>R_c\\ \zeta^{1/2}, & \zeta<R_c\end{cases}$$

where $\zeta=\dfrac{\rho y\upsilon}{\mu_{air}(T)}$ - Reynolds number, which is determined by the relative velocity of the gas to the wall, $\upsilon=\left|\vec{u}-\omega_{wall}\vec{k}\right|$ - gas velocity relative to the wall at a distance y from it, $u^*$ - dynamic velocity that is related to the tangential components of the stress tensor as follows:

$\vec{\sigma}_\omega-\left(\vec{\sigma}_\omega\cdot\vec{n}\right)\vec{n}=\rho\left(u^*\right)^2\dfrac{\vec{v}}{\upsilon}$, where $\vec{v}=\vec{u}-\omega_{wall}\vec{k}$, $k=\sqrt{c_\mu^{1/2}\left(c_{\varepsilon_2}-c_{\varepsilon_1}\right)\mathrm{Pr}_\varepsilon}$. The temperature value on the wall is fixed, therefore, the above-mentioned law of turbulence is used for it:

$$\frac{J_\omega}{\rho u^* c_p\left(T-T_\omega\right)}=\begin{cases}1/\left(\mathrm{Pr}_l\dfrac{\upsilon}{u^*}\right), & \zeta\le R\\ 1/\left\{\mathrm{Pr}\left[\dfrac{\upsilon}{u^*}+\left(\dfrac{\mathrm{Pr}_l}{\mathrm{Pr}}-1\right)R_c^{1/2}\right]\right\}, & \zeta>R_c\end{cases}$$

Where Pr - Prandtl number for laminar flow.

For the kinetic energy of turbulence $k$ and its dissipation rate $\varepsilon$, the following boundary conditions are written:

$\nabla k\cdot\vec{n}=0,\ \varepsilon=c_{\mu_\varepsilon}\dfrac{k^{3/2}}{y},\ c_{\mu_\varepsilon}=\left[\dfrac{c_\mu}{\mathrm{Pr}_\varepsilon\left(c_{\varepsilon_2}-c_{\varepsilon_1}\right)}\right]^{1/2}$, where $C_\mu$ is constant and its value is 0.09.

We have studied ($C_{14}H_{30}$) tetradecane's combustion depending on the Reynolds numbers of the gas flow. Tetradecane is the main component of diesel fuel. It's used in passenger, freight and private vehicles. Liquid fuel is injected into the combustion chamber through a circular nozzle, located in the center of the bottom of the chamber. The overview of the combustion chamber is presented in Fig.1.

The chamber is a cylinder with height equal to 15 cm and diameter is 0,04 m. After the injection there is a rapid evaporation of fuel and the combustion is processing in the gas phase. The burning time of fuel is $4\cdot10^{-3}$ s. Time of injection of fuel droplets is $1.4\cdot10^{-3}$ s. The temperatures of the walls of the combustion chamber is 353 K. The initial temperature of gas in the chamber is 900 K. The temperature of the injected fuel is 300 K. The initial mean radius of injecting drops is $3\cdot10^{-6}$ m. The pressure in the combustion chamber is $4.10^6$ Pa.

In the work the dependence of maximum temperature of fuel combustion from Reynolds numbers has been obtained. Reynolds numbers of the gas flow was ranging from 2300 to 25000. It has been known that at low velocities of liquid fuel spray the process of combustion does not occur [27-30].

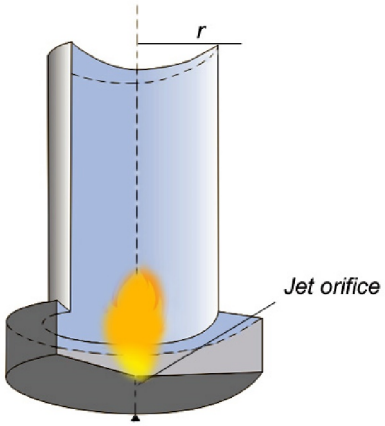


**Fig.1.** Overview of the combustion chamber

Tetradecane has been an object of research and its chemical formula has the following form as $C_{14}H_{30}$. For this type of fuel the global chemical reaction of combustion leading to the formation of carbon dioxide and water is written in the following way:

$$2C_{14}H_{30}+43O_2\rightarrow 28CO_2+30H_2O.$$

This reaction is exothermal, i.e. it proceeds with huge emission of heat.

In this scientific work the KIVA-II computer software package was used as the starting material which was developed by scientists at the Los Alamos National Laboratory (LANL). With this software package can explore the complex

processes of ignition, combustion of fuel and air mixtures, as well as the formation of pollutants released into the atmosphere as a result of the operation of internal combustion engines [18].

In this article, the KIVA-II software package has been optimized to simulate the chemical kinetics of combustion processes in diesel and aircraft engines. This software package was adapted to the task of combustion of liquid fuels in combustion chambers under high turbulence. This made it possible to calculate the aerodynamics of the flow, the injection masses, the oxidant's temperature, pressure, turbulent characteristics, concentrations of combustion products, fuel vapors and other characteristics of the process of liquid fuels' combustion over the entire space of the combustion chamber.

In this paper, the authors carried out simulation of combustion of liquid fuel in a cylindrical combustion chamber at different Reynolds numbers. Also similar computational experiments can be carried out for any kind of fuel. For example, in the following papers the authors carried out simulation of combustion of energy fuel in industrial boilers of Kazakhstan [31-36].

## NUMERICAL SIMULATION RESULTS

As the result of the conducted numerical experiments it has been determined that at high Reynolds numbers the combustion process occurs intensively. The most effective combustion proceeds at the Reynolds number of the gas flow equal 25000, under these conditions temperature reaches values from 2001 K to 2645 K (Fig.2).

Analysis of Fig.2 shows that if the Reynolds number of the flow in the combustion chamber takes values above 15000, then the fuel burns more intensively, a large amount of heat is generated and the combustion chamber warms up to 3000 K.

However Fig.3 shows the dependence of the distribution of $CO_2$ concentration on the Reynolds numbers of the flow, where the highest concentration of $CO_2$ is equal $0.106303 \cdot 10^{-3}$ kg/kg accounts for the Reynolds number of the flow Re=25 000.

But at the Reynolds numbers equal to 2300 $CO_2$ concentration reaches the minimum value to $0.103538 \cdot 10^{-3}$ kg/kg. Also, with a Reynolds numbers of 15 000 and 20 000, the concentrations of emitted carbon dioxide are relatively small, which are equal to $0{,}104823 \cdot 10^{-3}$ kg/kg and $0{,}104747 \cdot 10^{-3}$ kg/kg respectively. At these values of the Reynolds number, the fuel quickly reacts with an oxidizing agent, as a result, the concentration of carbon dioxide formed does not exceed the permissible limits.

Similar studies were conducted by scientists in the field of modeling of heat and mass transfer in the combustion chamber during combustion of solid fuels, especially coal. Many scholars who specialize in the field of computational fluid dynamics and heat power engineering conducted similar researches in the modeling of the combustion of liquid and solid fuels. In their works by the authors was used chemical model of pulverized coal combustion, which takes into account the integral component of the fuel oxidation reaction to the stable final products of the reaction. This model is the formation of the final products of oxidation is also used by us in the research [37-39].

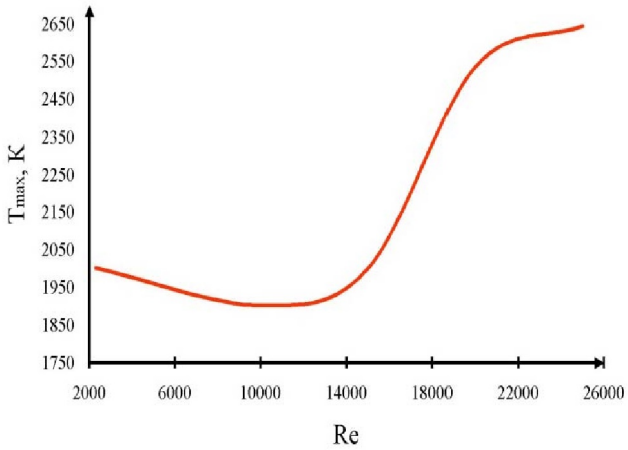


**Fig.2.** Change of maximum temperature in the burner chamber depending on the Reynolds numbers of the gas flow

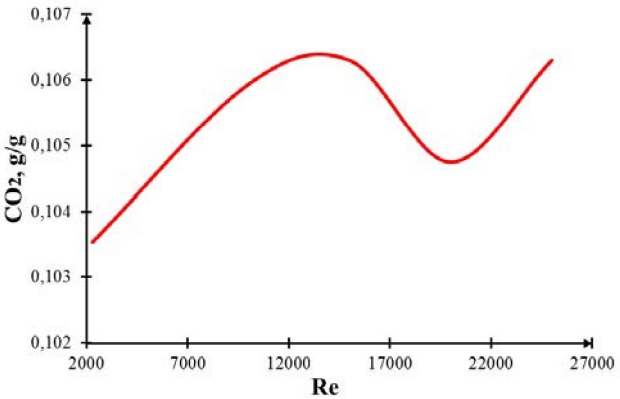


**Fig.3.** The dependence of the distribution of $CO_2$ concentration on the Reynolds number

For the optimum and maximum Reynolds number equal to 25000, the plots of the temperature

change in time and of the fuel concentration in the burner chamber have been obtained.

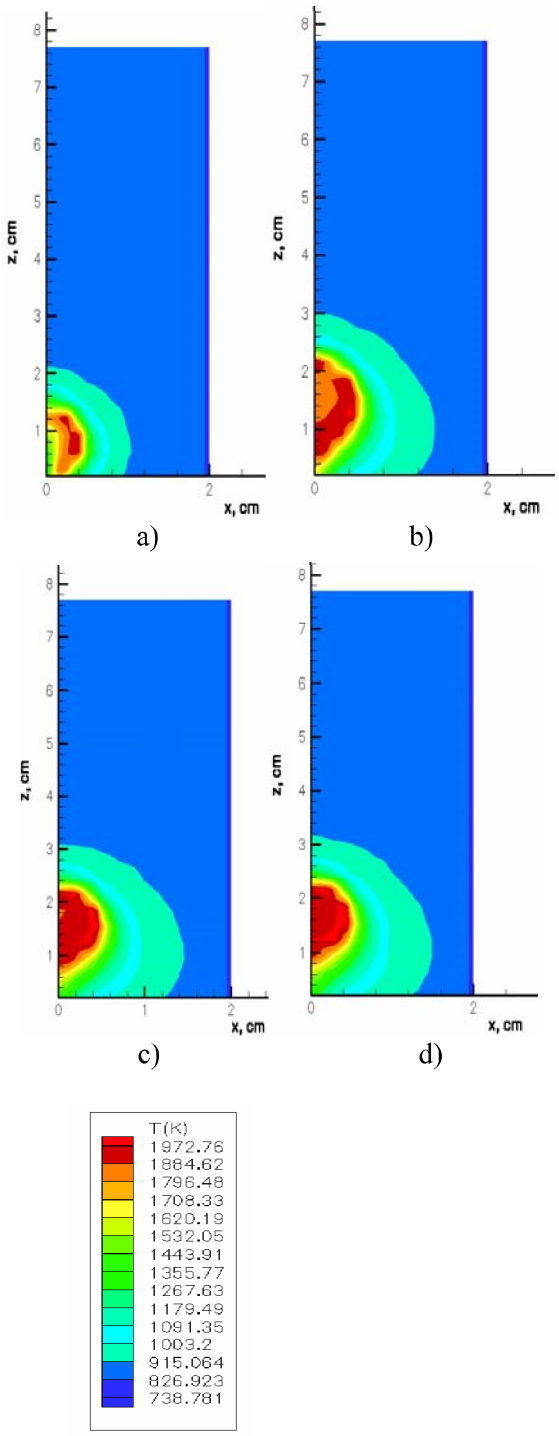


**Fig.4.** The temperature distribution in the combustion chamber during combustion of tetradecane at various time moments: a) $1.1 \cdot 10^{-3}$ s, b) $1.8 \cdot 10^{-3}$ s; c) $3 \cdot 10^{-3}$ s, d) $4 \cdot 10^{-3}$ s for the Re=25000

The following figures show the results of a computational experiment on the influence of the Reynolds number on the processes of atomization and combustion of liquid fuel (tetradecane). These graphs were obtained at an optimal value of the Reynolds number in the combustion chamber, equal to 25 000.

Fig.4 shows the distribution of the temperature in the space of the burner chamber for the Reynolds numbers equal to 25000 at different times: $1.1 \cdot 10^{-3}$ s, $1.8 \cdot 10^{-3}$ s, $3 \cdot 10^{-3}$ s, $4 \cdot 10^{-3}$ s correspondingly.

From these graphs (Fig.4) it can be seen how the temperature changes in the combustion chamber at different times. As can be seen from Fig.4, during the combustion of the tetradecane, the region of maximum temperatures at time $t=1.8 \cdot 10^{-3}$s reaches 0,022 m in height of the combustion chamber, the rest of the chamber is heated to 915 K. At this time, the mixture of fuel vapor with the oxidant is ignited, the fuel begins to burn rapidly, a large part of the width of the chamber is covered by thermal flame, where it reaches a value of the order of 1900 K.

At the final time moment the temperature reaches 2645 K and it can be seen that the temperature torch fills up almost all of the space of the chamber.

The distribution of the fuel concentration is presented in Fig.5 for the same time moments as for the temperature and for the Reynolds number 25000. At the initial moment the concentration of fuel has minimal value and then increases because of the fuel injection in the chamber. At high turbulence region occupied by the fuel in the chamber is reduced, a moment of time $t=1.8 \cdot 10^{-3}$s the fuel vapor of the tetradecane is raised to 0,03 m by the chamber axis.

The fuel quickly vaporizes, the vapors are mixed with the oxidant and the mixture ignites and burns down for $4 \cdot 10^{-3}$ s. At the final moment, the tetradecane burns without residue, the concentrations of fuel are almost zero.

Figs.6-7 show the dynamics of the distribution of reaction products concentration on time for the Reynolds number 25000. Analysis of the Fig.6 shows that with the maximum Reynolds number the maximum amount of carbon dioxide for tetradecane is formed on the axis of the combustion chamber and is equal to $0.114 \cdot 10^{-3}$ kg/kg. At the exit from the combustion chamber, the concentration of carbon dioxide decreases and takes the minimum values for tetradecane $0.008 \cdot 10^{-3}$ kg/kg.

Analysis of Fig.7 shows that at the time point of $4 \cdot 10^{-3}$ s the maximum concentration of water formed as a result of the chemical reaction of tetradecane's combustion is

$0.049 \cdot 10^{-3}$ kg/kg.

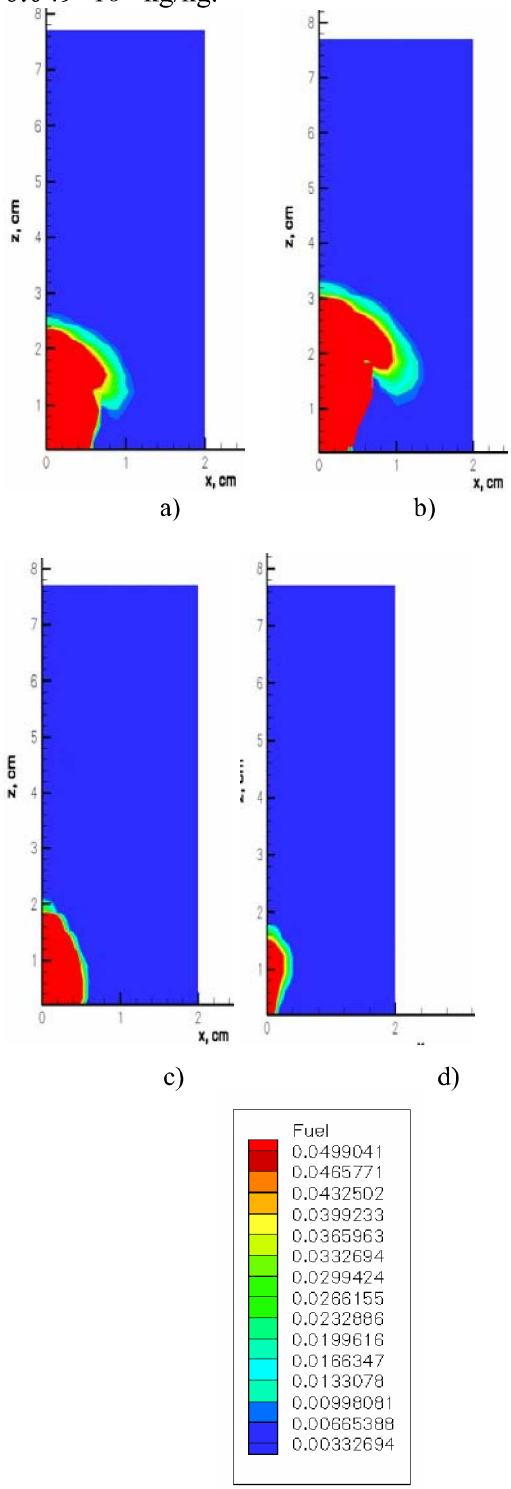


**Fig.5.** The distribution of fuel vapor concentration in the burner chamber at different time moments: a) $1.1 \cdot 10^{-3}$ s, b) $1.8 \cdot 10^{-3}$s; c) $3 \cdot 10^{-3}$ s, d) $4 \cdot 10^{-3}$s for the Re=25000

In other parts of the combustion chamber water concentration reaches the lowest value, which amounted to 0.0033 10-3 kg/kg. The values of the concentration of water are especially important in calculations related to the weight and volume of fuel, wherein the weight ratio of the amount of fuel to the weight of the same volume of water the fuel specific gravity is determined at a given temperature.

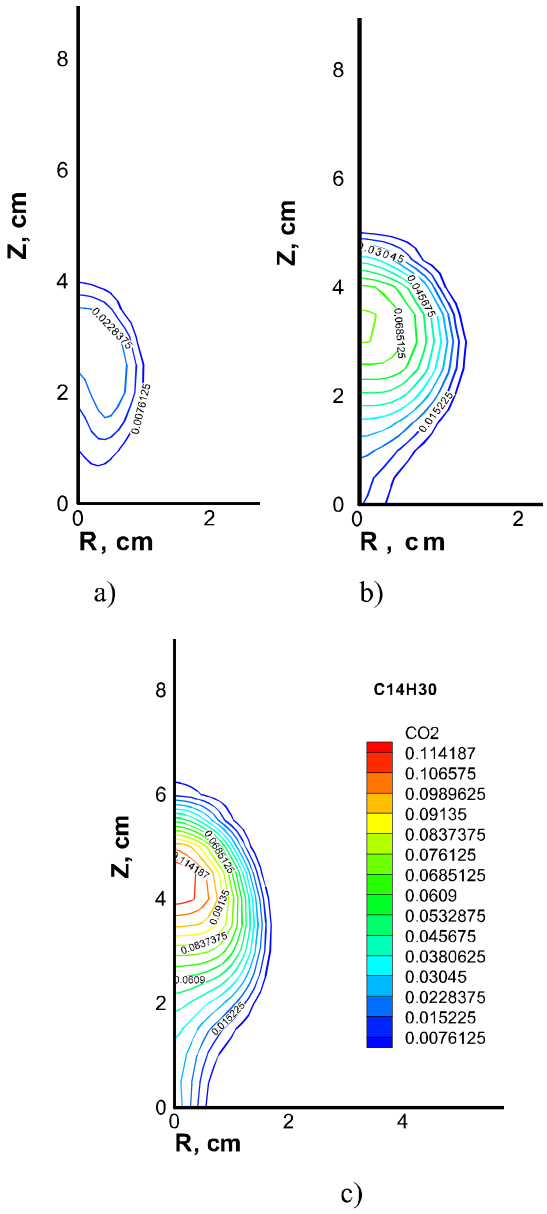


**Fig.6.** The distribution of $CO_2$ in the combustion chamber during combustion of tetradecane at various ·time moments: a) $1.1 \cdot 10^{-3}$ s, b) $1.8 \cdot 10^{-3}$ s; c) $3 \cdot 10^{-3}$ s, d) $4 \cdot 10^{-3}$ s for the Re=25000

The following Figs.8-10 show the results of computational experiments on the change in the temporal distributions of the Sauter mean droplet diameter (SMD) of tetradecane with distance from the injector. The Sauter mean diameter is the average volume-surface diameter of the droplets. It

also compares the results obtained with the experimental data presented by the authors *Arcoumanis C., Cutter P., Whitelaw D.* [40]. As can be seen from the figures, the calculated data and experimental data for dodecane are in good agreement.

In [40] studies were performed at various distances from the injector: $10 \cdot 10^{-3}$ m, $20 \cdot 10^{3}$ m, $30 \cdot 10^{-3}$ m, $40 \cdot 10^{-3}$ m, $50 \cdot 10^{-3}$ m and $60 \cdot 10^{-3}$ m for diesel fuel for Re=25000.

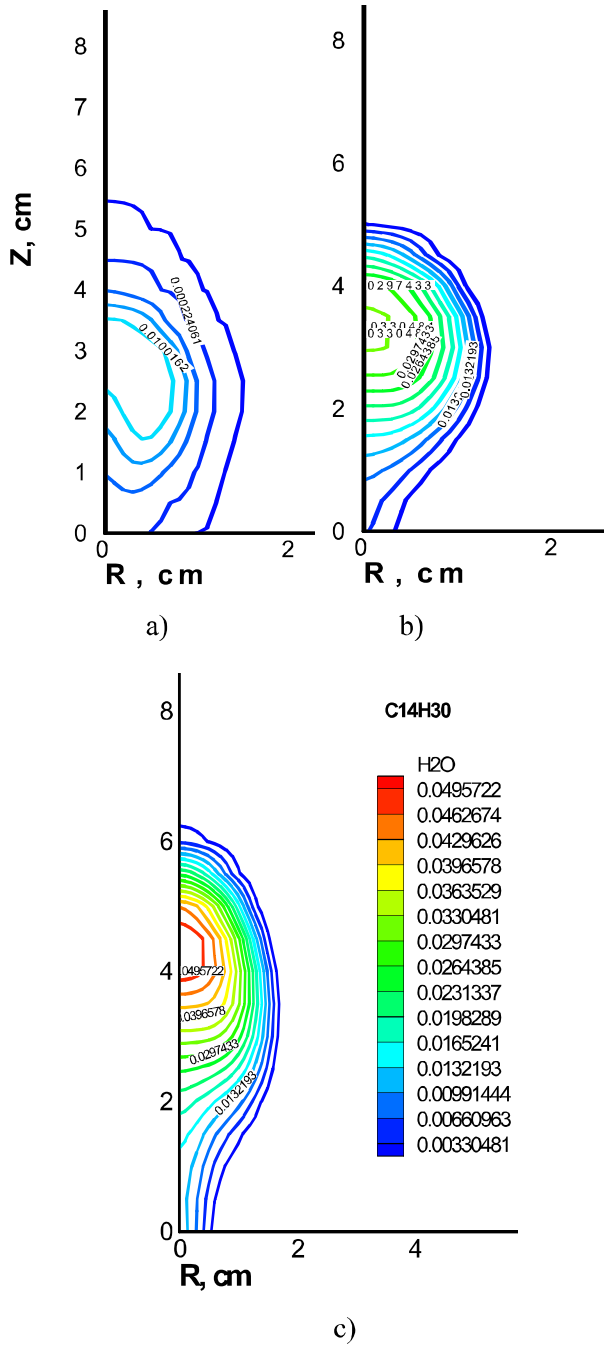


**Fig.7.** The distribution of concentration of $H_2O$ in the combustion chamber at time moments: ) $1.1 \cdot 10^{-3}$ s, b) $1.8 \cdot 10^{-3}$ s; c) $3 \cdot 10^{-3}$ s, d) $4 \cdot 10^{-3}$ s for the Re=25000

In this work a similar study at a distance of x = $30 \cdot 10^{-3}$ m, $40 \cdot 10^{-3}$ m, $50 \cdot 10^{-3}$ m and $60 \cdot 10^{-3}$ m from the injector for tetradecane and octane are conducted. Octane is the main component of gasoline. As can be seen from Figs.8-10, the coincidence of the data from the field and computer experiments is quite good. Analyzing the data obtained, it can be assumed that the calculated data and experimental data are in good agreement.

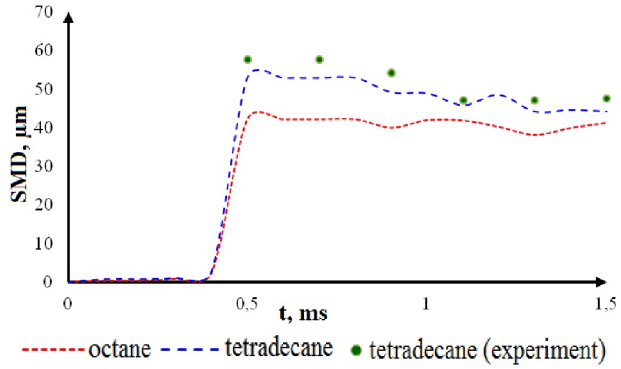


**Fig.8.** Comparison of the temporal distributions of the Sauter mean diameter of the tetradecane's droplet (SMD) at distances of $40 \cdot 10^{-3}$ m from the injector with experiment for the Re=25000

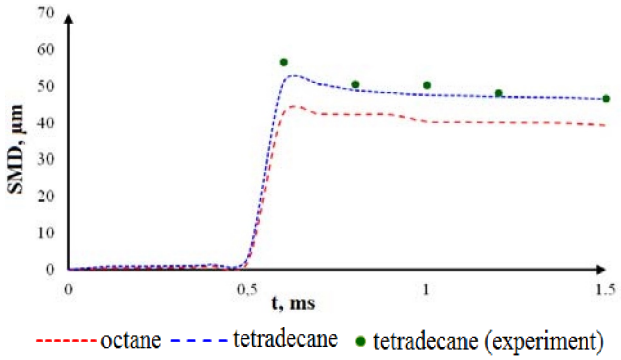


**Fig.9.** Comparison of the temporal distributions of the Sauter mean diameter of the tetradecane's droplet (SMD) at distances of $50 \cdot 10^{-3}$ m from the injector with experiment for the Re=25000

As can be seen from the figures, the results of computer simulation for tetradecane and experimental data for diesel fuel obtained by the authors [40] are in good agreement. The discrepancy in the results for octane can be explained by the fact that this element is found most of all in the composition of gasoline, the surface tension of which is much less than that of diesel fuel.

An analysis of the results presented in Figs.8-10 suggests a good agreement between the numerical

results and the experimental data and allows us to conclude that the numerical model for spraying liquid fuels proposed in the paper adequately describes the actual spray processes and, therefore, the process of burning various types of liquid fuels.

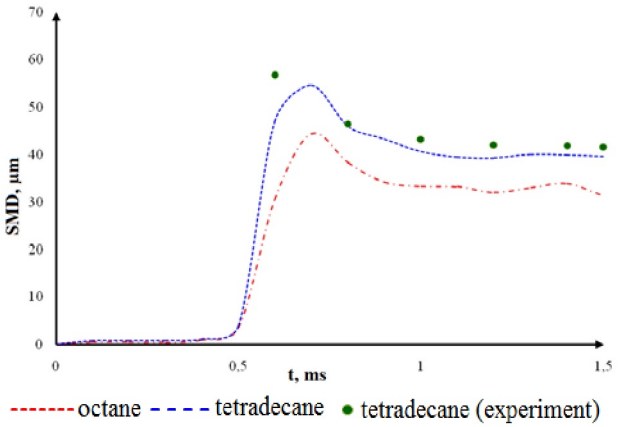


**Fig.10.** Comparison of the temporal distributions of the Sauter mean diameter of the tetradecane's droplet (SMD) at distances of $60 \cdot 10^{-3}$ m from the injector with experiment for the Re=25000

## CONCLUSIONS

In this work the influence of the Reynolds number of gas flow on tetradecane's combustion has been studied.

The distributions of maximum temperature and of $CO_2$ concentration depending on the Reynolds number, time distributions of the fuel, $CO_2$, $H_2O$ concentrations and temperature of the gas in the burner chamber for the effective Reynolds number have been obtained. Also the change of maximum temperature in the burner chamber depending on the Reynolds number of the gas flow has been obtained.

As a result of a computer study, the effective mode of the combustion process was determined. The most effective combustion proceeds at the Reynolds number of the gas flow equal 25000, under these conditions temperature reaches high values (from 2001 K to 2645 K).

At this temperature, the fuel is combusted completely, the chamber is warmed to a sufficiently high temperature, and the concentration of formed carbon dioxide takes the smallest value (to $0.104 \cdot 10^{-3}$ kg/kg).

Analyzing the distribution of the fuel vapor it can be concluded that the initial time vapor concentration was $0.05 \cdot 10^{-3}$ kg/kg than then at a final stage of the process of burning fuel vapor at the outlet from the combustion chamber was $0{,}003 \cdot 10^{-3}$ kg/kg.

Also, the results of numerical simulations were compared with experimental data, obtained by various authors. The temporal distributions of the Sauter mean diameter of the drops at different distances from the injector were obtained. The results of numerical simulation in this case was given a good agreement with experiment. Also for comparison of characteristics of various liquid fuels combustion processes has been studied two types of fuels. Verification of obtained during the computational results of the experiments, a comparison with experimental data and theoretical calculations have revealed good agreement.

The further study of the combustion of liquid sprays will let not only to develop methods for the decrease the contain of harmful substances in the atmosphere and prevention of formation of polluting fog, but also to improve the work of the engines of the internal combustion, of rockets, aviation engines and to make them more efficient and ecologically safer.

## REFERENCES

[1] Messerle, V. E., Ustimenko, A.B., etc. Numerical simulation of pulverized coal combustion in a power boiler furnace. *High temperature* **53** (3) 445-452 (2015).

[2] Bekmukhamet, A, Beketayeva, M.T. Gabitova, Z. K. etc. Computational method for investigation of solid fuel combustion in combustion chambers of a heat power plant. *High temperature* **5** (5) 751-757 (2015).

[3] Askarova, A. S., Bolegenova, S.A., Maximov, V.Y., etc. Numerical research of aerodynamic characteristics of combustion chamber BKZ-75 mining thermal power station. *Procedia Engineering* **42** 1250-12-59 (2012).

[4] Ospanova Sh., Gabitova Z., etc. Using 3D modeling technology for investigation of conventional combustion mode of BKZ-420-140-7c combustion chamber. *J. of Engineering and Applied Sciences* **9** (1) 24-28 (2014).

[5] Bolegenova S.A., etc. Mathematical simulation of pulverized coal in combustion chamber. *Procedia Engineering* **42,** 1259-1265 (2012).

[6] Boraiko C., Beardsley T., Wright E. Accident Investigations: one element of an effective safety culture. *Professional Safety* **53(9)**, 26-30 (2008).

[7] Clarke S. Safety climate in an automobile manufacturing plant: The effects of work environment, job communication and safety attitudes on accidents and unsafe behavior. *Personnel Review* **35(4),** 413-430 (2004).

[8] Dawal S.Z., Taha Z. The effects of job organizational factors on job satisfaction in two

automotive industries in Malaysia. *Journal of Human Ergo logy* **36(2),** 63-68 (2007).

[9] Dietl H., Royer S., Stratmann U. Value creation architectures and competitive advantage: lessons from the European automotive industry. *California Management Review* **51**, 24-28 (2009).

[10] Liang-Hung L., Iuan-Yuan L. Product quality as a determinant of product innovation: an empirical analysis of the global automotive industry. *Total Quality Management and Business Excellence* **14(2),** 141-147 (2006).

[11] Oh J., Rhee S.K. Influences of supplier capabilities and collaboration in new car development on competitive advantage of carmakers. *Management Decision* **48(5),** 756-774 (2010).

[12] Renard L. The automobile manufacturers' global competitiveness and dimension effects: Differentiation and cost advantages reconciled. *International Journal of Automotive Technology and Management* **2(3,4),** 280-288 (2002).

[13] Richardson M., Danford A., Stewart P., Pulignano V. Employee participation and involvement: Experiences of aerospace and automobile workers in the UK and Italy. *European Journal of Industrial Relations* **16(1),** 21-37 (2006).

[14] Sako M. The nature and impact of employee «voice» in the European car components industry. *Human Resource Management Journal* **8(2),** 5-13 (1998).

[15] Dadach Z.E. Cost Effective Strategies to Reduce CO2 Emissions in the UAE: A Literature Review. *Journal of Industrial Engineering and Management* **2(4),** 1-9 (2013).

[16] Smith M., Crotty J. Environmental regulation and innovation driving ecological designing the UK automotive industry. *Business Strategy and the Environment* **17 (6)**, 341-349 (2008).

[17] Gorokhovski, M., Chtab-Desportes, A., Voloshina, I., Askarova A. Stochastic simulation of the spray formation assisted by a high pressure. *AIP Conference Proceedings Xian*, **1207**, 66-73 (2010).

[18] Amsden, A.A., O'Rourke, P.J., Butler, T.D. KIVA-II: A computer program for chemically reactive flows with sprays. Los Alamos, 160. 1989.

[19] R. Manatbayev, Zh. K. Shortanbayeva, A. N. Aldiyarova, etc. Mathematical modeling of heat and mass transfer in the presence of physical-chemical processes. *Bulgarian Chemical Communications* **E**, 272-277 (2016).

[20] I. Berezovskaya, Sh. Ospanova, A. Nugymanova, etc. 3D modelling of heat and mass transfer processes during the combustion of liquid fuel. *Bulgarian Chemical Communications* **E**, 229-235 (2016).

[21] Beketayeva M., Ospanova Sh., etc. Investigation of turbulence characteristics of burning process of the solid fuel in BKZ 420 combustion chamber. *WSEAS Transactions on Heat and Mass Transfer* **9**, 39-50 (2014).

[22] Askarova A.S., Maximov Yu.V., Gabitova Z. K., etc. Numerical modeling of turbulence characteristics of burning process of the solid fuel in BKZ-420-140-7c combustion chamber. *Int. J. of Mechanics* **8**, 112-122 (2014).

[23] Bolegenova S.A., Beketayeva M.T., etc. Numerical experimenting of combustion in the real boiler of CHP. *Int. J. of Mechanics* **7,** 343-352 (2013).

[24] Lavrichsheva, Ye.I., Leithner, R., Müller, H., Magda, A., etc. Combustion of low-rank coals in furnaces of Kazakhstan coal-firing power plants. *VDI Berichte*, 497-502 (2007).

[25] Vockrodt S., Leithner. et al. Firing technique measures for increased efficiency and minimization of toxic emissions in Kasakh coal firing. *VDI, 19th German Conference on Flames, Germany, VDI Gesell Energietechn; Verein Deutsch Ingn., Combustion And Incineration, VDI Berichte* **1492**, 93, (1999).

[26] Askarowa A, Buchmann M.A. Structure of the flame of fluidized-bed burners and combustion processes of high-ash coal. *Gesell Energietech, Combustion and incineration - eighteenth dutch-german conference on flames, VDI Berichte*, **1313**, 241-244 (1997).

[27] Bolegenova, S.A., Bekmukhamet, A, etc. Control of Harmful Emissions Concentration into the Atmosphere of Megacities of Kazakhstan Republic. *Int. Conf. on Future Information Engineering (FIE2014), IERI Procedia, Beijing, China* 252-258 (2014).

[28] A. Yergaliyeva, A. Boranbayeva, K. Berdikhan, etc. Application of 3D modelling for solving the problem of combustion coal-dust flame. *Bulgarian Chemical Communications* **E**, 236-241 (2016).

[29] E. I. Heierle, A. B. Ergalieva, etc. CFD study of harmful substances production in coal-fired power plant of Kazakhstan. *Bulgarian Chemical Communications* **E**, 260-265 (2016).

[30] R. Leithner, Sh. Ospanova, etc. Computational modeling of heat and mass transfer processes in combustion chamber at power plant of Kazakhstan. *MATEC Web of Conferences* DOI:10.1051/ matecconf/ 20167606001, 1–5 (2016).

[31] Karpenko, E. I., Karpenko, Yu. E., Messerle, V. E., Ustimenko, A. B., etc. Mathematical modelling of the processes of solid fuel ignition and combustion at combustors of the power boilers. *7th Int. Fall Seminar on Propellants, Explosives and Pyrotechnics Xian* **7**, 672-683 (2007).

[32] Askarova A., Bolegenova Symbat, Ergalieva A., etc. 3D modeling of heat and mass transfer during combustion of solid fuel in BKZ-420-140-7c combustion chamber of Kazakhstan. *J. of Applied Fluid Mechanics* 699-709 (2016).

[33] Messerle V. E., Ustimenko A.B., etc. Reduction of noxious substance emissions at the pulverized fuel combustion in the combustor of the BKZ-160 boiler of the Almaty heat electropower station using the "Overfire Air" technology. *Thermophysics and aeromechanics* **23** (1) 125-134 (2016).

[34] Berdikhan, K., etc. Application of numerical methods for calculating the burning problems of coal-dust flame in real scale. *Int. J. of Applied Engineering Research* **11** (8) 5511-5515 (2016).

[35] Askarova A., Bolegenova S. et al. Influence of boundary conditions to heat and mass transfer processes. *Int. J. of Mechanics* **10**, 320-325 (2016).

[36] Maximov V. et al. On the effect of the temperature boundary conditions on the walls for the processes of heat and mass transfer. *Int. J. of Mechanics* **10**, 349-355 (2016).

[37] Askarova, A. S., Maksimov, V. Yu., et. al. Numerical simulation of the coal combustion process initiated by a plasma source. *Thermophysics and aeromechanics* **21**, (6) 747-754 (2014).

[38] Karpenko E. I., Messerle V.E. et al. Plasma enhancement of combustion of solid fuels. *J. of High Energy Chemistry* **40**, (2) 111-118 (2006).

[39] Beketayeva, M., Safarik, P., et al. Numerical Modeling of Pulverized Coal Combustion at Thermal Power Plant Boilers. *J. of thermal science* **24** (3) 275-282 (2015).

[40] Arcoumanis C., Cutter P., Whitelaw D. S. Heat transfer processes in diesel engines. *Institution of Chemical Engineer Trans IChemE* 70, 124-132 (1998).

*Bulgarian Chemical Communications, Volume 50, Special Issue G (pp. 7 8 - 85 ) 2018*

# Atmospheric dispersion modelling and radiological safety analysis for a hypothetical accident of liquid-fuel thorium molten salt reactor (TMSR-LF)

Bo Cao[1, 2, 3*], Weijie Cui[1, 2], Irsa Rasheed[1, 2], Yixue Chen[1, 2]

[1]*School of Nuclear Science and Engineering, North China Electric Power University, Beijing, 102206, China*

[2]*Beijing Key Laboratory for Passive Safety Technology of Nuclear Energy, North China Electric Power University, Beijing, 102206, China*

[3] *Departments of Atmospheric and Oceanic Sciences, University of California, Los Angeles, CA, 90095, USA*

The molten salt reactor (MSR) is one of the six advanced reactor types for future nuclear energy proposed in the Generation IV International Forum (GIF). Because of its potentially favourable economic, fuel utilization, and safety characteristics and nuclear proliferation resistance, the MSR has aroused widespread concern in recent years. Indeed, from 2011, the Shanghai Institute of Applied Physics started the "Thorium Molten Salt Reactor Nuclear Energy System (TMSR)" project in China and aimed to construct a liquid-fuel thorium molten salt reactor (TMSR-LF) and a solid-fuel thorium molten salt reactor (TMSR-SF). An optimized 2 MWth TMSR-LF has been designed and will be built recently in Gansu province. In this study, HotSpot health physics computer code has been used for atmospheric dispersion modelling and radiological safety assessment considering site-specific meteorological conditions. Calculations for total effective dose equivalent (TEDE), ground deposition and the respiratory time-integrated air concentration have been performed, with results indicating maximum value of ground deposition equal to 2.5E+01kBq/m$^2$at a distance of 0.6km from the reactor. Maximum value of TEDE falls below the public dose limit of 1mSv/year proposed by ICRP even for the worst case accident scenario as set in IAEA safety Report Series number 115. The TEDE has three components: inhalation, ground shine and air submersion, the submersion and ground shine doses are insignificant compared to the inhalation doses. It is observed that the highest value of committed effective dose equivalent (CEDE) appears to be the lung, the lower large intestine wall appears to be the second most exposed organ, followed by upper large intestine wall and the red marrow, respectively. The contribution of total 18 selected radionuclides was investigated, three main radionuclides including Sr-90, Sr-89, Cs-137 are the main contributors to the CEDE.

**Keywords:** atmospheric dispersion modelling, radiological safety analysis, TMSR-LF, TEDE, HotSpot

## INTRODUCTION

Generation IV International Forum (GIF) has anticipated molten salt reactor (MSR) as one of the advanced reactors to fulfil the future nuclear energy demands [1], owing to its economic fuel utilization, nuclear proliferation resistance and advanced safety characteristics [2-6].

The MSR was first developed in the Oak Ridge National Laboratory (ORNL) in the late 1940s. The first Molten Salt Reactor Experiment (MSRE) began to construct in 1962 and operated at full power in December 1966 [7]. Several conceptual designs of the MSR have been proposed and have been studied in the past 60 years. Japan, Russia and other countries also paid much attention to the MSR [4, 8-10]. In China, the Shanghai Institute of Applied Physics started the "Thorium Molten Salt Reactor Nuclear Energy System (TMSR)" project in China and aimed to construct a liquid-fuel thorium molten salt reactor (TMSR-LF) and a solid-fuel thorium molten salt reactor (TMSR-SF).

An optimized 2 MWth TMSR-LF has been designed and will be built in Gansu province recent years. For a MSR, as a fluid fuel reactor, on-line fuel processing can be applied, which helps in removal of gaseous and volatile parts from the source term [7, 11]. The MSR is a more safety advanced reactor and is more resistant to consequences of large accidents in comparison to other reactor types, but there is risk for the source term may be released to the environment [3-5]. It is still necessary to predict the radiological safety analysis of a hypothetical accident with the radionuclides available for release to the environment.

Radiological safety analysis for hypothetical accident provides a major contribution for the safety analysis of nuclear power plant, as far as human health and safety is concerned [12-20].

The total effective dose equivalent (TEDE) attributes to both internal and external dose equivalents for the body resulting from the release of radionuclides during accident. Thus, TEDE is computed by addition of both effective dose equivalent (EDE) and the total committed effective dose equivalent (CEDE). The EDE was caused by the external material such as submersion, ground shine and resuspension, and CEDE was caused by

* To whom all correspondence should be sent:
caobo@nccpu.edu.cn

the internal material such as inhalation. The TEDE is the most complete expression of the combined dose from all applicable delivery pathways [20, 21].

Lawrence Livermore National Laboratory (LLNL) has established a HotSpot computer code for the analysis of personnel health physics near the reactor sites. Gaussian Plume Model (GPM) has been employed for HotSpot code for the calculation of air concentration and TEDE due to release of radionuclides into the atmosphere [21]. In practice, the GPM is one of the most widely validated general dispersion models and has been successfully applied in various dispersion problems [13-20].

In this work, we have performed the atmospheric dispersion modelling and radiological safety analysis of a hypothetical TMSR-LF accident by HotSpot health physics computer code considering site-specific meteorological conditions. The TEDE, the respiratory time-integrated air concentration, and the ground deposition are calculated with source term including 18 radionuclides. These results provide reference for the assessment source term of emergency facility and offsite consequence assessment.

## MATERIALS AND METHOD

### *Site-specific conditions of the TMSR-LF*

The TMSR-LF will be in the Wuwei City, Gansu Province, China. It will be built about 2020. Wuwei city has a temperate continental arid climate, where evaporation is larger than precipitation. The local meteorological data indicate a mean year rainfall is about 60~610 mm and a mean year evaporation is about 1400~3040 mm. North-North-West (NNW) and West-South-South (WSS) are the predominant directions, which occurred for about 49.1% and 10.4% with an average speed of 5.0m/s and 2.0m/s, respectively. Stability class D gains predominance as it has percentage occurrence of 61.2%, the second being the stability class E with percentage occurrence of 9.3%, and the remaining 29.5% is taken by other classes.

### *Source term and accidental release scenario*

The TMSR-LF is a graphite moderated reactor. The thermal power is 2 MW, and the fuel salt is $LiF\text{-}BeF_2\text{-}ThF_4\text{-}UF_4$ (68-28-0.1-3.9 mol %) with 99.95 % abundance of $^7Li$ and a coolant salt of LiF-NaF-KF [2, 6].

Although MSR has some inherent features compared with other reactor systems, it still has some safety disadvantage, including the accumulation of fission products in different parts like the primary system, the off-gas system, the fuel storage tanks, and the processing plant. This highlights the significance for proper containment of fission products and removal of decay heat under all anticipated circumstances [11]. According to the research, off-gas system failure accident is generally recognized as the most likely path for radiation release [4, 5]. Base on it, in this paper, the source term is mainly contributed by the off-gas system failure and the radioactivity leak by reactor vessel and pipes. The accident source term during 0~ 1 hour for TMSR-LF is shown in Tab.1 [6].

**Table 1:** Accident source term for TMSR-LF

| Nuclide | Activity released / Bq |
|---|---|
| H-3 | $3.30\times10^{12}$ |
| Kr-85 | $8.75\times10^{4}$ |
| Kr-85m | $1.28\times10^{6}$ |
| Kr-87 | $1.45\times10^{7}$ |
| Kr-88 | $1.03\times10^{7}$ |
| Xe-133 | $2.48\times10^{4}$ |
| Xe-135 | $4.17\times10^{6}$ |
| I-131 | $1.51\times10^{7}$ |
| I-132 | $2.83\times10^{6}$ |
| I-133 | $3.54\times10^{7}$ |
| I-134 | $1.15\times10^{8}$ |
| I-135 | $6.96\times10^{8}$ |
| Cs-134 | $4.21\times10^{6}$ |
| Cs-137 | $1.63\times10^{10}$ |
| Sr-89 | $5.29\times10^{11}$ |
| Sr-90 | $8.46\times10^{10}$ |
| Ru-103 | $8.38\times10^{5}$ |
| Ru-106 | $1.89\times10^{5}$ |

The release height was assumed at 40 m and buoyancy and exit momentum effects were neglected. Depending on the site meteorology, a downwind transportation of radionuclides happens after the accident. The annual average wind speed at 10 m is 5 m/s in the predominant direction of NNW. Stability class D gains predominance because of its largest percentage occurrence of 61.2%, a default value of 1.7m for the receptor height and value of 1300m for the inversion layer height has been chosen. A value of $3.33\times10^{4}$ $m^3$ s/l